When Light Falls in LOV: A Quantum Mechanical/Molecular Mechanical Study of Photoexcitation in Phot-LOV1 of *Chlamydomonas reinhardtii*

Markus Dittrich,[†,‡] Peter L. Freddolino,[†,§] and Klaus Schulten*[,†,‡]

Beckman Institute, Department of Physics, and Center for Biophysics and Computational Biology, University of Illinois at Urbana−Champaign, 405 North Mathews Avenue, Urbana, Illinois 61801

Received: February 23, 2005; In Final Form: April 26, 2005

Plants use sophisticated photosensing mechanisms to maximize their utilization of the available sunlight and to control developmental processes. The plant blue-light receptors of the Phot family mediate plant phototropism and contain two light, oxygen, and voltage (LOV)-sensitive domains as photoactive elements. Here, we report combined quantum mechanical/molecular mechanical simulations of the photocycle of a complete Phot-LOV1 domain from *Chlamydomonas reinhardtii*. We have investigated the electronic properties and structural changes that follow blue-light absorption. This permitted us to characterize the pathway for flavin−cysteinyl adduct formation, which was found to proceed via a neutral radical state generated by hydrogen atom transfer from the reactive cysteine residue, Cys57, to the chromophore flavin mononucleotide. Interestingly, we find that adduct formation does not cause any larger scale conformational changes in Phot-LOV1, which suggests that dynamic effects mediate signal transmission following the initial photoexcitation event.

1. Introduction

The conversion of sunlight into energy storage by the photosynthetic apparatus of plants is ubiquitous, and its importance for all of life cannot be overemphasized. However, in addition to the ability to efficiently store light energy, organisms have to be able to respond to light cues from their environment, e.g., to adjust to changes in light conditions and to avoid damaging overexposure to light. Photosynthetic organisms have met these requirements by evolving sophisticated photosensing mechanisms. The responsible photoreceptors are the red-light-sensitive phytochromes[7] and the blue-light receptors of the cryptochrome and phototropin family.[6]

The plant phototropin family comprises Phot1 and Phot2,[3−5] which mediate light-induced responses such as phototropism,[8,9] stomatal opening and closing,[30] chloroplast relocation,[25,26] and gametogenesis.[21] Both Phot1 and Phot2 have two nonidentical light, oxygen, and voltage (LOV)-sensing domains, LOV1 and LOV2, as photoactive elements on the N-terminal side and a serine−threonine kinase moiety on the C-terminal side. The LOV domains are members of the well-characterized PER-ARNT-SIM[42] family of sensor proteins that bind noncovalently the chromophore flavin mononucleotide (FMN).

Spectroscopically, there are significant differences in the photochemical properties of LOV1 and LOV2, e.g., in regard to their quantum efficiencies and photoproduct decay times. Insight into the function of LOV domains has been gained through the determination of X-ray crystallographic structures of phy3-LOV2 from *Adiantum capillus-veneris*[11,12] and of Phot-LOV1 from the algae *Chlamydomonas reinhardtii*.[16]

For the Phot-LOV1 domains of *C. reinhardtii*, experimental studies have provided a detailed characterization of its photocycle. Upon excitation of the chromophore FMN into an excited singlet state, fast intersystem crossing (ISC) on the time scale of a few nanoseconds leads to an excited triplet state absorbing in the red at 715 nm.[31] This triplet state then decays over the course of ∼4 μs into a blue-shifted species absorbing at 390 nm that is thought to represent a flavin−cysteinyl adduct between the C4a atom of FMN and the sulfur of a nearby cysteine residue, Cys57. This adduct is long-lived and decays on a time scale of several seconds to minutes back to the original dark state.

The authors of ref 16 solved the structure of both the dark and the light states of Phot-LOV1 in *C. reinhardtii*, the latter evolving from the former upon light irradiation. The atomic-resolution structures provided clear evidence for a flavin−cysteinyl adduct in the illuminated state, thereby confirming spectroscopic data. Furthermore, these structures allowed the interpretation of the roles played by specific protein residues located close to the chromophore, particularly in terms of their possible influence on the photoreaction itself. Important for our purposes is the fact that the relatively high resolution at which both structures were determined establishes an ideal starting point for computer simulations.

Several computational studies of the electronic properties of flavins, including lumiflavin, have been reported in the literature. The authors of ref 16 conducted quantum chemical studies determining the change in electron distribution during the photocycle. Neiss et al. have performed ab initio calculations of the excited-state properties of flavin-related molecules and also conducted a model study of the first steps of the LOV domain's photocycle.[35] Recently, the authors of ref 36 reported a molecular dynamics (MD) study of the LOV2 domain from *A. capillus-veneris* that compared the dynamic behavior of the dark and light states of the system.

However, despite the availability of a significant amount of spectroscopic and structural data as well as, recently, computational results, we still lack a detailed understanding of the photocycle. Of particular interest is the pathway for flavin−

* Author to whom correspondence should be addressed. Phone: (217) 244-1604. Fax: (217) 244-6078. E-mail: kschulte@ks.uiuc.edu.
† Beckman Institute.
‡ Department of Physics.
§ Center for Biophysics and Computational Biology.

10.1021/jp050943o CCC: $30.25
Published on Web 06/15/2005

cysteinyl adduct formation, which is currently not very well characterized on an electronic level. In fact, several reaction mechanisms have been put forward. Swartz et al. proposed an ionic mechanism involving a thiolate anion and a cationic FMN that was assumed to be protonated by one of the amino acid residues in the binding pocket.[41] This suggestion was later refuted by infrared spectroscopy.[1] The authors of refs 13 and 16 proposed a concerted mechanism in which proton transfer from the cysteine to FMN-N5 is accompanied by nucleophilic attack of the thiolate anion onto FMN-C4a. Kennis et al.[29] suggested that the initial proton transfer from the cysteine to FMN-N5 is a separate event that is then followed by nucleophilic attack of the sulfur on FMN-C4a. Finally, the authors of refs 32 and 39 proposed a radical-pair mechanism for adduct formation via either electron transfer or movement of a hydrogen atom from the cysteine to the FMN moiety and subsequent bond formation after ISC has taken place. On a more macroscopic scale, it is at present not known how flavin−cysteinyl adduct formation in LOV is coupled to the signaling action of the whole Phot protein.

Here, we report combined quantum mechanical/molecular mechanical (QM/MM) simulations of the photocycle of the Phot-LOV1 domain of *C. reinhardtii* that allowed us to resolve the structural changes and electronic processes accompanying flavin−cysteinyl adduct formation. We have investigated the LOV1 ground and flavin−cysteinyl adduct state as well as several intermediates in the triplet excited state occurring during the photocycle. Our simulations provide electronic level insight into the reaction pathways, and we find the adduct-formation reaction to be of the radical-pair type.

2. Methods

System Preparation. The simulations reported here are based on the dark state crystal structure of Phot-LOV1 in *C. reinhardtii* by Fedorov et al.[16] solved at 1.9-Å resolution (PDB code 1N9L). All water molecules as well as a sulfate ion present in the original structure were removed and missing hydrogen atoms were added to the FMN−protein complex. The monophosphate group of FMN was chosen to be deprotonated and, therefore, has a net charge of $-2e^-$. The complex was then solvated in a 32.6-Å sphere of 6024 TIP3P water molecules, yielding a final system size of 19 804 atoms and is shown in Figure 1.

The system was then minimized and equilibrated for 2.4 ns in the *NVT* ensemble with the molecular dynamics program NAMD2[27] and the AMBER94[10] force field. The parameters employed for the FMN part of the system were the ones developed by Schneider et al.[40] During minimization and equilibration, spherical boundary conditions as implemented in NAMD2 were used to preserve the overall system shape and prevent the evaporation of water molecules. To obtain a properly minimized structure, the system was then subjected to further simulated cooling from 298 K to a final temperature of 20 K in steps of 10 K and an equilibration time of 40 ps per cycle followed by 500 000 steps of conjugate gradient minimization using NAMD2. In all subsequent QM/MM simulations, the spherical boundary conditions were replaced by fixing all water molecules in a shell extending from a radius of 28 Å to the exterior of the water sphere at 32.6 Å. The system was then subjected to further minimization using a steepest descent algorithm until a final gradient smaller than 10^{-5} hartree/bohr was reached.

QM/MM Simulations. The classically optimized structure described above provided the starting configuration for a series of QM/MM simulations. The quantum mechanically treated core

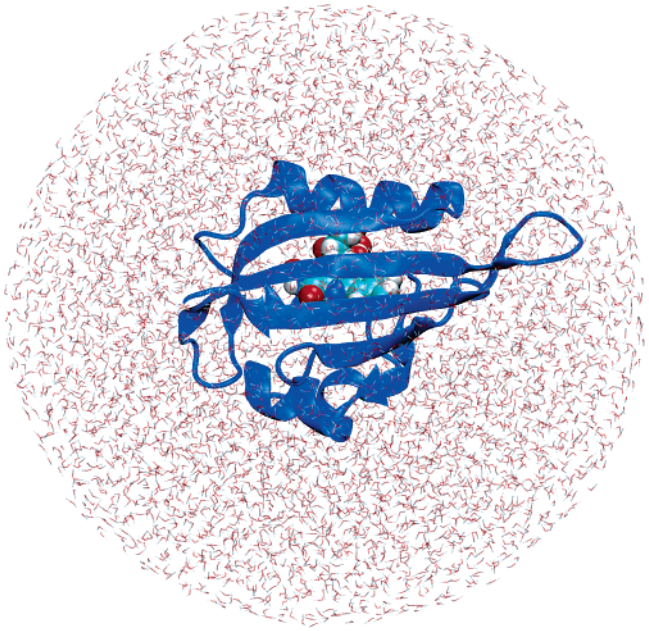

Figure 1. LOV1 domain simulation system. Shown is the Phot-LOV1 protein in cartoon representation with the FMN chromophore depicted as van der Waals spheres located inside the binding pocket. Also shown is the solvation sphere consisting of 6024 TIP3P water molecules.

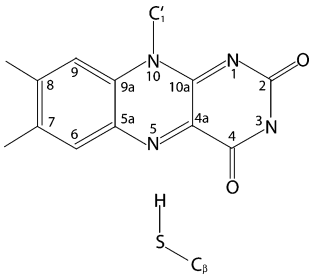

Figure 2. QM core region. Shown is a schematic view of the quantum mechanically treated core region, consisting of the lumiflavin part of FMN and the side chain of Cys57. The figure also provides the atom numbering used in the remainder of the paper.

segment is shown in Figure 2 and encompasses the lumiflavin part of FMN up to the C1′ atom of the ribityl chain and the side chain of Cys57 up to C_β.

The frontier orbitals at the boundary between the quantum and the classical regions were treated using the link-atom approach, and the free valences were capped with hydrogen atoms. Our QM/MM interface uses a RESP charge algorithm for the electrostatic coupling between the quantum and the classical regions and is described in detail in refs 19 and 20. All geometry optimizations and single-point calculations of the singlet and excited triplet states were conducted using a Hartree−Fock (HF) description at the RHF/6-31G(2d,2p) and ROHF/6-31G(2d,2p)[14,15,17,22] levels of theory, respectively. The use of restricted open-shell HF (ROHF) wave functions for the triplet excited states was necessary since the unrestricted HF wave functions exhibited a significant degree of spin contamination (>25%). To further corroborate our HF results, all calculations reported here with the exception of the transition state determination were repeated using density functional theory (DFT) at the B3LYP/6-31G(d) and U-B3LYP/6-31G(d) levels of theory and were found to be in excellent qualitative agreement with our HF data. However, since the triplet excited state belongs to the same irreducible representation as the singlet ground state, the DFT approach is, formally, not rigorously defined, and we therefore report the HF results only.

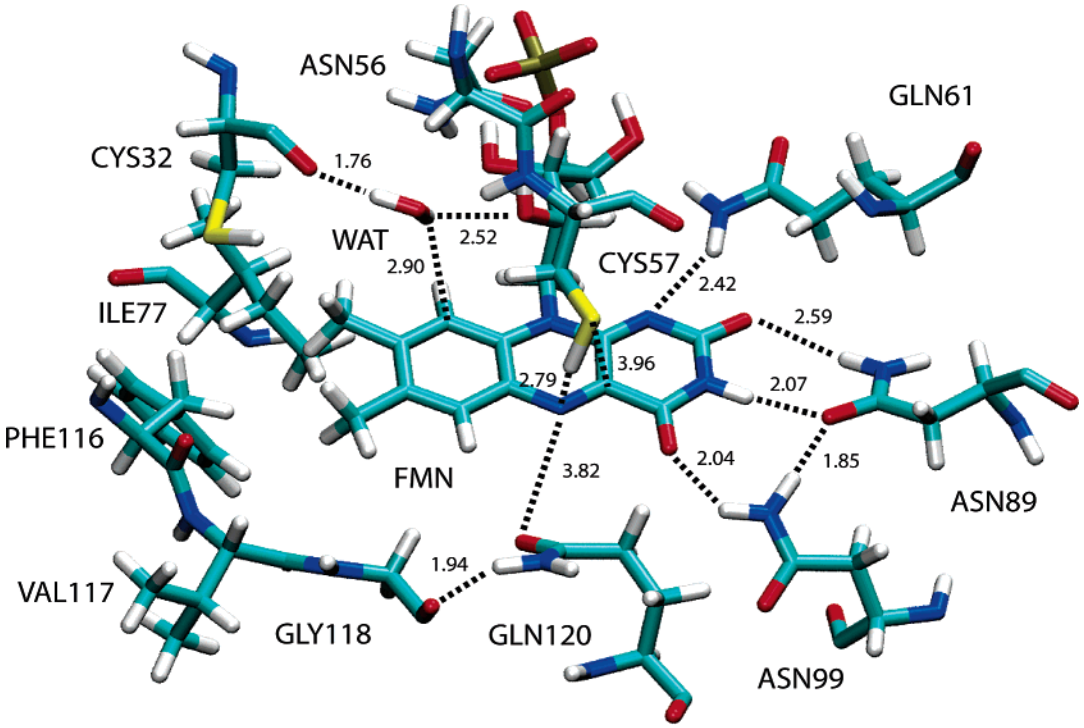

Figure 3. FMN binding pocket. Shown are the FMN chromophore and the residues of the LOV protein lining the binding pocket together with key interatomic distances in Å.

All geometry optimized conformations were confirmed to be true minima by calculating the Hessian matrix and analyzing its eigenvectors.

The transition state between T_1 and $T_{radical}$ was determined via constrained optimizations along the approximate reaction coordinate for hydrogen transfer given by the Cys57-H−FMN-N5 distance vector. The resulting conformation was validated to be a true transition state by the presence of a single imaginary frequency in the Hessian matrix and intrinsic reaction coordinate calculations connecting the transition state to T_1 and $T_{radical}$, respectively. We did not, however, attempt to determine the transition state separating S_{adduct} and the singlet ground state, S_0.

3. Results

Here, we report our findings for the reaction pathway of flavin−cysteinyl adduct formation in Phot-LOV1 upon photoexcitation obtained via QM/MM simulations. We present the computational results that characterize the important states along this pathway in their proper reaction order.

FMN Binding Pocket Conformation. The structural organization of the binding pocket is shown in Figure 3, which depicts the FMN chromophore and residues lining the pocket. One can clearly discern the presence of polar residues adjacent to the pyrimidine side of FMN, whereas the dimethyl benzol ring is surrounded by nonpolar residues. During the initial classical equilibration phase, several water molecules migrated into the FMN binding pocket. The water molecule approaching the closest to the chromophore is hydrogen-bonded to Cys32 and the ribityl chain of FMN (cf. Figure 3) and, hence, too far away from the reactive thiol group to contribute to adduct formation. Interestingly, the equilibration causes the rotation of the side chain of Gln120 with respect to its position in the crystal structure such that eventually the amide oxygen is pointing toward FMN as opposed to the amide nitrogen in the original structure.

Singlet Ground State, S_0. Figure 3 depicts the conformation of FMN and several surrounding protein residues in the singlet ground state, S_0, i.e., before photon absorption has taken place. FMN's lumiflavin moiety is planar, forming three hydrogen bonds with protein side chains at its pyrimidine side, namely, Asn89-$O_{\delta 1}$−FMN-H3 (2.07 Å), Asn89-$H_{\delta 21}$−FMN-O2 (2.59 Å), and Asn99-$H_{\delta 21}$−FMN-O4 (2.04 Å). The sulfur of Cys57 is located almost directly above FMN-N5 with respect to the lumiflavin plane at a distance to FMN-C4a of 3.96 Å. The thiol hydrogen is pointing toward FMN-N5 and located 2.79 Å from the nitrogen atom. The intra-FMN bond lengths depicted in Figure 4 show that the N5−C4a bond has a double-bond character compared to the single N5−C5a bond, with bond orders of 1.67 and 1.13 for the two bonds, respectively (data not shown).

Triplet Reactant State, T_1. The triplet state T_1 is reached via intersystem crossing (ISC) and possible further vibrational relaxation from an excited singlet state S_n generated by photon absorption. As shown in Figure 4, at the ROHF/6-31G(2d,2p) level of theory, T_1 is energetically 50.77 kcal/mol above S_0.

To characterize the electronic character of this state further, Figure 5 depicts the highest occupied molecular orbitals (HOMOs) of S_0 and T_1. An examination of the respective molecular orbitals reveals that T_1 is of the $\pi-\pi^*$ type.

Table 1 lists the change in Mulliken charges with respect to S_0, revealing a shift of negative charge toward N5 that originates mostly from C5a and C4a. This shift is accompanied by lengthening of the N5−C4a bond (cf. Figure 4) from 1.27 to 1.36 Å due to a reduction in its double-bond character (bond order 1.15). At the same time, the N5−C5a bond contracts from 1.36 to 1.28 Å, caused by an increase in its double-bond character (bond order 1.60).

The increase in negative charge on the N5 nitrogen is accompanied by a slight movement of the thiol group toward FMN (by ~0.02 Å for Cys57-S) and leads to a slight increase in the charge of the thiol hydrogen itself. Apart from these

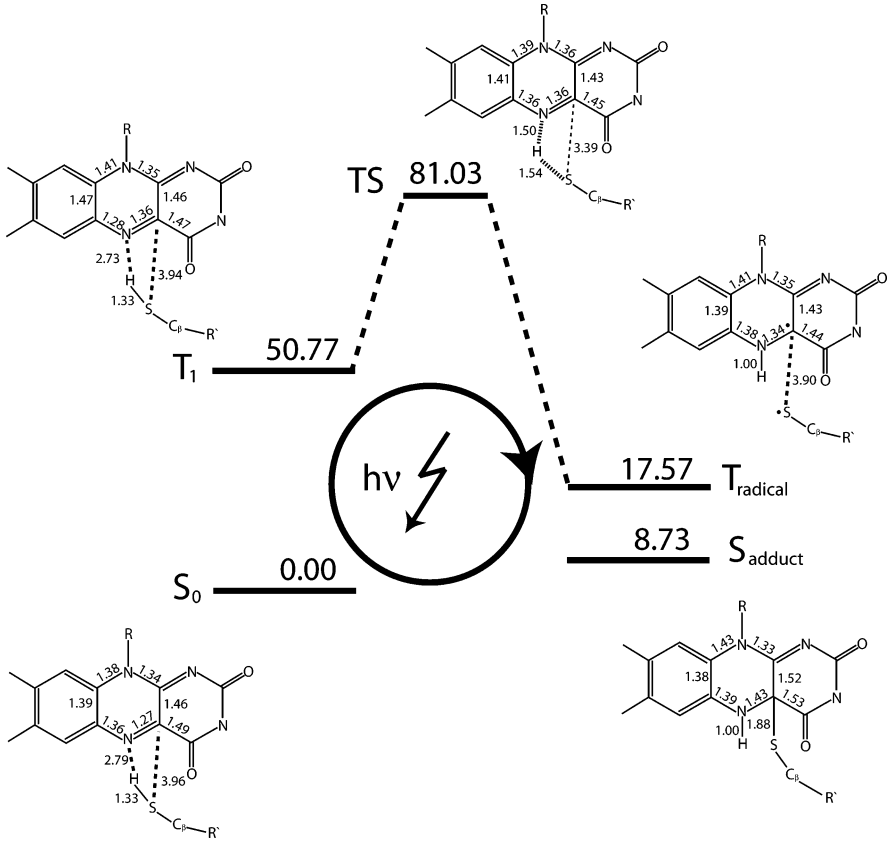

Figure 4. LOV1 photocycle. Shown is a schematic representation of the computed structures and energies of S_0, T_1, the transition state (TS), $T_{radical}$, and S_{adduct} determined at the RHF/6-31G(2d,2p) and ROHF/6-31G(2d,2p) levels of theory. Also shown are important bond lengths in Å.

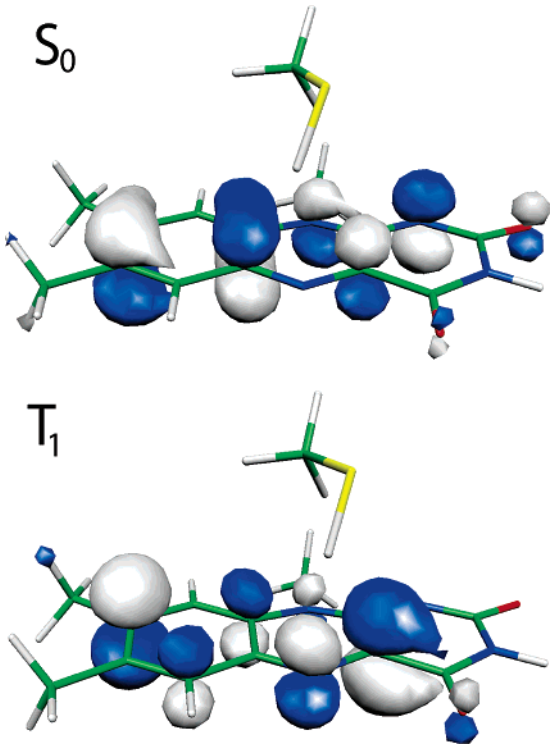

Figure 5. Highest occupied molecular orbitals. Depicted are the HOMOs of the quantum mechanically treated core region in S_0 and T_1 determined at the RHF/6-31G(2d,2p) and ROHF/6-31G(2d,2p) levels of theory, respectively. The HOMO of S_0 is a bonding π-orbital, that of T_1 an antibonding π^*-orbital.

charge rearrangement and structural changes involving the thiol group and the chromophore atoms C4a, N5, and C5a, our simulations reveal only minor differences between S_0 and T_1.

TABLE 1: Mulliken Charges on Important Atoms[a]

atom name	S_0	T_1	TS	$T_{radical}$	S_{adduct}
FMN-C4	0.00	0.00	0.01	−0.01	0.03
FMN-O4	0.00	0.00	−0.01	−0.07	−0.03
FMN-C4a	0.00	0.07	0.08	0.05	−0.13
FMN-N5	0.00	−0.14	−0.28	−0.13	−0.20
FMN-C5a	0.00	0.06	0.08	0.09	0.10
FMN-C9a	0.00	−0.03	0.03	−0.05	−0.06
FMN-C10a	0.00	0.01	0.04	0.01	0.02
Cys57-C_β	0.00	0.00	0.02	−0.01	−0.05
Cys57-S	0.00	−0.01	−0.20	0.04	0.17
Cys57-H	0.00	0.01	0.17		
FMN-H5				0.22	0.19

[a] Given are the changes in Mulliken charges with respect to S_0 of key atoms in FMN and Cys57 calculated at the RHF/6-31G(2d,2p) and ROHF/6-31G(2d,2p) levels of theory for S_0, T_1, the transition state (TS), $T_{radical}$, and S_{adduct}.

In the top panel of Figure 6, the most significant values for the atomic spin populations $\Delta\rho = \rho_\uparrow - \rho_\downarrow$ in the triplet reactant state T_1 are shown. Clearly, one observes a spin density that is distributed over most of the lumiflavin ring with no significant contribution by the thiol group, the largest share being provided by atoms C4a and C8.

Triplet Radical State, $T_{radical}$. Interestingly, our QM/MM simulations reveal the existence of a triplet state, $T_{radical}$, in which the thiol group hydrogen has transferred from Cys57-S to FMN-N5 and is now located 1.00 Å away from N5 in the lumiflavin plane. This is shown in Figure 4.

$T_{radical}$ evolved from T_1 via hydrogen transfer along a reaction coordinate given approximately by the Cys57-S−FMN-N5 distance vector. The conformation of the corresponding transition state structure is shown in Figure 4 and exhibits an energy of 81.03 kcal/mol; it is, therefore, ∼30 kcal/mol above T_1. Table 1 lists the Mulliken charges on important atoms in the transition

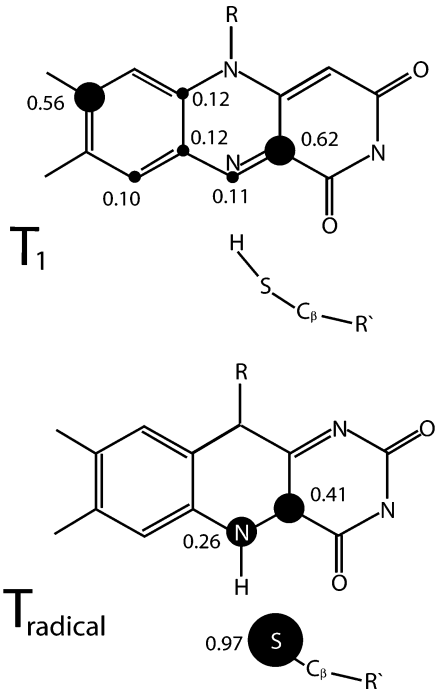

Figure 6. Mulliken spin populations. Shown are the atomic Mulliken spin populations $\Delta\rho_S = \rho_t - \rho_i$ for T_1 and $T_{radical}$. Only the contributions with $|\Delta\rho_S| \geq 0.1$ at the ROHF/6-31G(2d,2p) level of theory are given.

TABLE 2: Total Mulliken Charges on FMN and Cys57[a]

fragment	S_0	T_1	TS	$T_{radical}$	S_{adduct}
FMN[b]	0.01	0.01	0.08	0.01	−0.12
Cys57[c]	−0.01	−0.01	−0.08	−0.01	0.12

[a] Given are the total Mulliken charges on FMN and Cys57 calculated at the RHF/6-31G(2d,2p) and ROHF/6-31G(2d,2p) levels of theory for S_0, T_1, the transition state (TS), $T_{radical}$, and S_{adduct}. [a] FMNH for $T_{radical}$ and S_{adduct}. [b] Cys57 without hydrogen for $T_{radical}$ and S_{adduct}.

state and reveals a significant charge polarization between Cys57-H (+0.17e⁻), Cys57-S (−0.20e⁻), and FMN-N5 (−0.28e⁻).

Energetically, $T_{radical}$ was found 33 kcal/mol below the triplet reactant state but still 17 kcal/mol above the singlet ground state, S_0 (cf. Figure 4).

The observed movement of negative charge toward the N5 nitrogen in T_1 facilitates the hydrogen-transfer process. An analysis of the total Mulliken charge on FMN and Cys57 given in Table 2 clearly shows that $T_{radical}$ evolves from T_1 through transfer of a hydrogen atom as opposed to proton transfer and, therefore, constitutes a neutral radical species.

In this context, it is important to note that the triplet radical character of the electronic wave function in $T_{radical}$ represents an intrinsic property of the FMNH−Cys57-S system in the conformation studied by us. In other words, once hydrogen transfer has taken place, the triplet radical state corresponds to the electronic ground state with triplet spin symmetry of the system. Even though it might, in principle, be possible that a different structural arrangement of FMNH and Cys57-S leads to a wave function with, e.g., ionic character, we were not able to identify such a state. On the basis of our analysis, we do not find it likely that a state other than the neutral triplet radical observed in this study exists in the conformation of Phot-LOV1 studied by us.

Bond formation between FMN-N5 and the transferred thiol hydrogen atom pushes negative charge mostly toward FMN-O4, leading to an increased negative charge on this atom. Finally, an examination of the spin populations given in Figure 6 reveals a localization of the unpaired spin on FMN-C4a and N5 as well as, interestingly, the sulfur atom of Cys57.

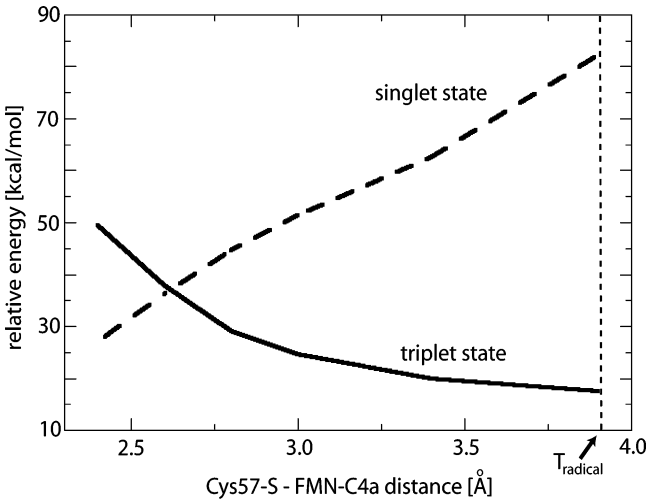

Figure 7. Energetics of triplet−singlet intersystem crossing. Shown are the approximate potential energy profiles measured with respect to S_0 of the triplet and singlet states in the neighborhood of $T_{radical}$. The latter is located at a Cys57-S−FMN-C4a distance of 3.90 Å.

To investigate the electronic properties of the singlet state coupled to $T_{radical}$ via ISC, we examined the triplet and singlet state potential energy surfaces in the vicinity of $T_{radical}$ by constrained optimizations along the approximate reaction coordinate for the transition from $T_{radical}$ to S_{adduct} given by the Cys57-S−FMN-C4a distance. This is shown in Figure 7. Even though a vertical transition at the $T_{radical}$ geometry yields a high-energy conformation of ∼82 kcal/mol, our calculations predict a much more moderate upper limit for the energy required to cross from the triplet to the singlet state potential energy surface of approximately 18 kcal/mol.

Singlet Flavin−Cysteinyl Adduct State, S_{adduct}. Figure 4 shows the conformation of the flavin−cysteinyl adduct state that evolves from the triplet excited state upon ISC to the singlet configuration. S_{adduct} was obtained from the conformation of $T_{radical}$ via geometry optimization after changing the multiplicity of the wave function, thereby establishing a direct connection on the potential energy surface between those two states (cf. Figure 7).

The previously planar lumiflavin part in the state S_{adduct} is now tetrahedrally distorted due to the sp^3 hybridization of C4a caused by bond formation between the carbon atom and Cys57-S. The newly formed carbon−sulfur bond has a length of 1.88 Å. However, due partly to the tetrahedral distortion of FMN, Cys57 approaches FMN only slighty, e.g., by ∼0.54 Å for the distance between Cys57-C_β and FMN-N10. Hence, the adduct formation does not lead to any significant structural changes beyond the distortion of FMN itself.

Energetically, the flavin−cysteinyl adduct state lies approximately 10 kcal/mol below $T_{radical}$ and 8 kcal/mol above S_0.

Excitation-Induced Protein Structural Changes. With the exception of FMN and the reactive Cys57 residue, the protein undergoes only very minor structural changes while traversing the four states of the photocycle described here, despite the fact that the protein is able to move freely inside the solvent sphere. This is clearly reflected in the root-mean-square deviations between the conformations of T_1, $T_{radical}$, and S_{adduct}, with respect to S_0; these are 0.00 Å (0.01 Å), 0.03 Å (0.08 Å), and 0.02 Å

(0.08 Å), respectively. Here, the numbers in parentheses denote the root-mean-square deviation for the complete protein including FMN, whereas the first number excludes FMN and the atoms of Cys57.

The protein conformational changes between S_0 and T_1 are completely confined to the lumiflavin ring and the thiol group of Cys57 described above. In $T_{radical}$, we observe a motion of the side chain of Gln120 toward N5 on the lumiflavin ring (cf. Figure 3). The distance between Gln120-O_ϵ and FMN-N5 decreases by 0.41 Å, caused by the transfer of the thiol hydrogen to the lumiflavin ring and the resulting positive charge on the hydrogen atom (cf. Table 1). Apart from this movement, there are no other significant changes in $T_{radical}$. Finally, in the flavin−cysteinyl adduct state, S_{adduct}, the major conformational change is again confined to the FMN ring and, due to bond formation, to residue Cys57. However, the secondary structural elements connected to Cys57 are only slightly affected. The side chain of Gln120 moves back toward its position in the reactant state and assumes a final position ∼0.21 Å from its initial state.

4. Discussion

Our computational findings provide new electronic level insight into the photocycle and into flavin−cysteinyl adduct formation in Phot-LOV1. The results are in good overall agreement with published experimental and theoretical data, and their implications for the mode of operation of this remarkable photosensor will be discussed below.

Energetics of the Phot-LOV1 Photocycle. From an energetic point of view, our results suggest the following order of events upon photon absorption in the singlet ground state, S_0. ISC from an excited singlet state relaxes the system into an excited triplet reactant state, T_1, that subsequently converts into a neutral triplet radical state, $T_{radical}$. A second ISC event then leads to triplet−singlet conversion followed by bond formation between the sulfur atom of Cys57 and FMN-C4a to yield a flavin−cysteinyl adduct state. The latter conformation eventually converts back to the singlet ground state.

At the ROHF/6-31G(2d,2p) level of theory, the energy of the excited triplet state is 50.77 kcal/mol above the singlet ground state. For lumiflavin in the gas phase, Neiss et al.[35,37] report a singlet−triplet splitting of 2.07 eV (47.7 kcal/mol) at the B3LYP/6-31G* level of theory. Hence, our results indicate that the presence of the protein environment does not give rise to a significant change in the singlet−triplet excitation energy compared to the gas phase. A value of ∼50 kcal/mol is also in good agreement with a recent energy content analysis of this state by Losi et al.[33] One can, therefore, conclude that the main role of the protein environment is the provision of a favorable arrangement of protein residues, particularly that of the reactive thiol group of Cys57, to facilitate bond formation rather than to change the overall reaction energetics. Using electron paramagnetic resonance (EPR), Schleicher et al.[39] arrived at a similar conclusion based on their observed small change in the zero-field splitting parameter $|D|$.

The triplet reactant state, T_1, then converts exothermically into a triplet radical species, $T_{radical}$, that will be discussed in more detail below. Energetically, the radical state is approximately 33 kcal/mol below the initial triplet state and, therefore, 17 kcal/mol above the singlet ground state. We were able to identify the reaction pathway linking T_1 and $T_{radical}$, even though the transition state barrier height of ∼30 kcal/mol is overestimated by our HF method.

ISC leads subsequently to triplet−singlet conversion and flavin−cysteinyl adduct formation. This step also proceeds exothermically, since our calculations predict an energy of 8 kcal/mol for the flavin−cysteinyl adduct state, which corresponds to ∼16% of the initial triplet excitation energy. Such a low-energy conformation of S_{adduct} is in agreement with a quantum chemical study of adduct formation for several FMN model compounds.[35] The latter study reports, e.g., an energy of 2.51 kcal/mol for the adduct state between 8-methyl lumazine and the molecule $HSCH_3$. A low-energy conformation for the flavin−cysteinyl adduct state is, however, in stark contrast to findings by Losi et al.[33,34] for YtvA-LOV and Phot-LOV1 of *C. reinhardtii*. These authors used laser-induced optoacoustic spectroscopy to probe the energy content of various intermediates of the LOV photocycle. They find that in both systems the flavin−cysteinyl adduct assumes a high-energy, strained conformation with an energy of 43 kcal/mol for Phot-LOV1. The analysis of protein structural changes observed during our simulations (cf. Results section) clearly shows that LOV does not assume any strained conformations since all structural changes are fully confined to the immediate vicinity of FMN. Furthermore, in light of the observed small structural differences between the X-ray crystal structures of the dark and the light states of LOV1 from *C. reinhardtii*,[16] it is unlikely that such a high-energy strained conformation could arise. The cause of this discrepancy between experimental and computational studies is unclear and deserves further investigation.

To complete the photocycle, a transformation of the flavin−cysteinyl adduct state to the initial singlet ground state needs to take place. According to our results (cf. Figure 4), this process is exothermic by ∼8 kcal/mol and will, therefore, proceed spontaneously with a rate constant determined by the height of the transition state barrier.

Triplet−Singlet Intersystem Crossing. A thorough analysis of the wave function for T_1 and $T_{radical}$ provides a clear picture of how triplet−singlet intersystem crossing in Phot-LOV1 is effected. The atoms that harbor a significant fraction of the unpaired spin are shown in Figure 6. A close look at the data shows that, initially, the unpaired spin is distributed over most of the lumiflavin plane. Furthermore, due to the absence of aromatic protein residues in the vicinity of the lumiflavin ring, the triplet state can be assumed to be confined to the chromophore itself, as suggested in ref 39 based on EPR studies. In this context, it would be interesting to conduct a study similar to the one reported here for LOV2, for which an X-ray crystal structure[11] revealed the presence of a phenylalanine residue in π-stacking distance just below the lumiflavin ring.

Upon formation of $T_{radical}$, the unpaired spin localizes on the atoms primarily involved in adduct formation, i.e., Cys57-S, FMN-C4a, and FMN-N5. These are ideal conditions for sulfur-generated ISC. Due to its strong spin−orbit coupling constant, the sulfur atom is able to initiate efficient triplet−singlet intersystem crossing of the nearby located unpaired spin,[2] leading to a rapid decay of the triplet radical state. The resulting short lifetime of $T_{radical}$ could explain why spectroscopically only a single triplet species, corresponding to T_1, without spectral evolution indicating the presence of $T_{radical}$ is observed.[29] Furthermore, the existence of such an efficient spin conversion channel in the triplet radical state suggests that ISC occurs before flavin−cysteinyl bond formation takes place. The ISC event then paves the way for bond formation between Cys57-S and FMN-C4a in the singlet state.

Adduct-Formation Pathway. The mechanism for flavin−cysteinyl adduct formation has been hotly debated in the literature, and several different pathways have been proposed. Initially, adduct formation was suggested to proceed via a

thiolate anion and a cationic FMN,[41] protonation/deprotonation of which was proposed to be due to protein residues located nearby. Such an ionic mechanism, however, has been refuted based on experimental data[1,24] and was, therefore, not investigated here. A neutral and protonated thiol group and a neutral and unprotonated FMN were assumed as initial states in all of our simulations.

Three additional mechanisms have been invoked to explain flavin−cysteinyl adduct formation in LOV domains. An ionic mechanism has been suggested[13,29] that involves proton abstraction from the thiol group by FMN-N5 in the excited triplet state followed by nucleophilic attack of the thiolate on the C4a position of FMN.

On the basis of their crystal structure of phy3-LOV2 from *A. capillus-veneris* in the dark state, Crosson et al.[11] proposed a concerted mechanism for adduct formation in which FMN-N5 is protonated while the thiol sulfur carries out a nucleophilic attack onto the C4a position. Similarly, Fedorov et al.[16] suggest a concerted mechanism based on their crystal structures for Phot-LOV1 of *C. reinhardtii* and theoretical Mulliken charge distributions obtained via quantum chemical calculations.

Our QM/MM simulations of the photocycle in Phot-LOV1 identify a third mechanism as the relevant pathway for flavin−cysteinyl adduct formation in Phot-LOV1: a radical-pair mechanism as shown by the neutral radical state $T_{radical}$ (cf. Table 1) that evolves from T_1 via hydrogen atom transfer from the thiol group of Cys57 to FMN-N5.

The energy of the transition state separating T_1 and $T_{radical}$ was found to be ∼80 kcal/mol above S_0, corresponding to a barrier height of ∼30 kcal/mol with respect to T_1. In light of the experimentally measured transition times from the triplet toward the adduct state, which are on the microsecond time scale, this barrier is clearly too high. This could be due to the chosen HF method, which might not be able to properly describe the electronic wave function at the transition state conformation. However, we cannot rule out the presence of other lower-energy transition state conformations connecting T_1 and $T_{radical}$.

Analysis of the Mulliken charge distribution calculated for the transition state structure (cf. Table 1) suggests that the hydrogen atom is transferred from the cysteine to FMN via a coupled proton−electron transfer rather than that of a hydrogen radical. Such a hydrogen-transfer process is also in accord with the $\pi-\pi^*$ character of T_1 and gives rise to the observed radical-pair state $T_{radical}$.

A radical-pair mechanism has also been suggested by the optical and EPR spectroscopy of Kay et al.[28] and Schleicher et al.[39] and by the quantum chemical simulations of flavin−cysteinyl adduct formation between isolumazine and $HSCH_3$ of Neiss et al.[35] In principle, such a radical mechanism can evolve either via electron transfer from the thiol group to FMN giving rise to a zwitterionic radical species or via transfer of the thiol hydrogen yielding a neutral radical. On the basis of their data, Schleicher et al.[39] favor a zwitterionic radical species whereas Neiss et al.[35] find that a neutral radical mechanism proceeding via hydrogen atom transfer is energetically most favorable. Our results agree with the latter view, but it is evident that this triplet radical state deserves further experimental and theoretical investigation.

Constrained optimizations along the approximate reaction coordinate for adduct formation given by the Cys57-S−FMN-C4a distance provided an upper limit for the barrier height of 18 kcal/mol with respect to $T_{radical}$ for the crossing between the triplet and the singlet potential energy surfaces. Hence, even though the true barrier may be significantly lower, dynamic effects can be expected to play a role in the ISC event between $T_{radical}$ and S_{adduct}, e.g., fluctuation-driven shortening of the Cys57-S−FMN-C4a distance.

Protein Structural Changes. One of the central questions of LOV1 function is the coupling of its photocycle to the kinase activity of the full phototropin protein, which eventually relays the excitation by light to the signaling activity of Phot-LOV1 in *C. reinhardtii*. A comparison of the structures for the dark and light states of LOV1 in *C. reinhardtii*[16] reveals that all significant conformational changes are confined to the region immediately surrounding FMN. However, genetic analysis and comparison of available crystal structures for different species led Crosson et al.[13] to suggest a series of interconnected residues extending from FMN to the outside of the protein to be responsible for signal transduction. Our simulations support the findings of Federov et al.[16] since they do not reveal any significant structural changes beyond the immediate vicinity of FMN and the reactive residue Cys57 (cf. Results section). It has to be kept in mind, however, that our QM/MM approach is not able to overcome barriers separating local minima on the potential energy surface, which might be necessary to allow for such larger structural changes. The signaling to the kinase domain of the protein could, e.g, be mediated by interactions with the surface of the LOV1 domain that are altered through slight rearrangements of the FMN moiety in the protein core, possibly involving secondary structural elements such as the β-sheet of LOV domains or the J_α-helix suggested by Harper et al.[18] for the Phot1-LOV2 domain of *Avena sativa.*

5. Conclusions

Here, we report the results of an ab initio QM/MM study of the photocycle in the Phot-LOV1 domain of *C. reinhardtii*. Our calculations provide structures, energies, and electronic properties of important states traversed during the photocycle of Phot-LOV1. Our findings shed light on the nature of the exited triplet state, and flavin−cysteinyl adduct formation is found to proceed via a neutral triplet radical species. The accumulation of the unpaired spin in $T_{radical}$ close to the thiol sulfur of Cys57 primes the system for efficient and fast triplet−singlet intersystem crossing and likely is the reason why such a radical state has so far eluded experimental investigation. Surprisingly, all conformational changes observed during the photocycle are confined to the chromophore itself and protein residues in its immediate vicinity. This can be taken as further evidence for the suggestion that photoinduced signal transmission is not due to conformational changes of the LOV1 domain itself but rather caused by a change in its dynamic properties resulting from covalent bond formation between Cys57 and FMN and a likely small but significant shift of FMN in its binding pocket.

Acknowledgment. The molecular images in this paper were created with the molecular graphics program VMD[23] with exception of Figure 5, which was created using Molekel.[38] We thank the Pittsburgh Supercomputer Center for continuous support and acknowledge the use of their GS1280 computational facilities made available by the National Center for Research Resources (RR06009). This work is supported by grants from the National Institutes of Health (PHS-5-P41-RR05969) and the National Science Foundation (MCB02-34938). The authors gladly acknowledge supercomputer time provided by Pittsburgh Supercomputer Center and the National Center for Supercomputing Applications via the National Resources Allocation Committee (MCA93S028).

References and Notes

(1) Ataka, K.; Hegemann, P.; Heberle, J. Vibrational spectroscopy of an algal Phot-LOV1 domain probes the molecular changes associated with blue-light reception. *Biophys. J.* **2003**, *84*, 466−74.

(2) Bittl, R.; Kay, C. W. M.; Weber, S.; Hegemann, P. Characterization of a flavin radical product in a C57M mutant of a LOV1 domain by electron paramagnetic resonance. *Biochemistry* **2003**, *42*, 8506−12.

(3) Briggs, W. R.; Christie, J. M. Phototropins 1 and 2: Versatile plant blue-light receptors. *Trends Plant Sci.* **2002**, *7*, 204−10.

(4) Briggs, W. R.; Beck, C. F.; Cashmore, A. R.; Christie, J. M.; Hughes, J.; Jarillo, J. A.; Kagawa, T.; Kanegae, H.; Liscum, E.; Nagatani, A.; Okada, K.; Salomon, M.; Rüdiger, W.; Sakai, T.; Takano, M.; Wada, M.; Watson, J. C. The phototropin family of photoreceptors. *Plant Cell* **2001**, *13*, 993−7.

(5) Briggs, W. R.; Christie, J. M.; Salomon, M. Phototropins: A new family of flavin-binding blue light receptors in plants. *Antioxid. Redox Signaling* **2001**, *3*, 775−88.

(6) Briggs, W. R.; Huala, E. Blue-light photoreceptors in higher plants. *Annu. Rev. Cell Dev. Biol.* **1999**, *15*, 33−62.

(7) Briggs, W. R.; Olney, M. A. Photoreceptors in plant photomorphogenesis to date. Five phytochromes, two cryptochromes, one phototropin, and one superchrome. *Plant Physiol.* **2001**, *125*, 85−8.

(8) Christie, J. M.; Briggs, W. R. Blue light sensing in higher plants. *J. Biol. Chem.* **2001**, *276*, 11457−60.

(9) Christie, J. M. Salomon, M.; Nozue, K.; Wada, M.; Briggs, W. R. LOV (light, oxygen, or voltage) domains of the blue-light photoreceptor phototropin (nph1): Binding sites for the chromophore flavin mononucleotide. *Proc. Natl. Acad. Sci. U.S.A.* **1999**, *96*, 8779−83.

(10) Cornell, W. D.; Cieplak, P.; Bayly, C. I.; Gould, I. R., Jr.; Merz, K. M.; Ferguson, D. M.; Spellmeyer, D. C.; Fox, T.; Caldwell, J. W.; Kollman, P. A. A second generation force field for the simulation of proteins, nucleic acids, and organic molecules. *J. Am. Chem. Soc.* **1995**, *117*, 5179−5197.

(11) Crosson, S.; Moffat, K. Structure of a flavin-binding plant photoreceptor domain: Insights into light-mediated signal transduction. *Proc. Natl. Acad. Sci. U.S.A.* **2001**, *98*, 2995−3000.

(12) Crosson, S.; Moffat, K. Photoexcited structure of a plant photoreceptor domain reveals a light-driven molecular switch. *Plant Cell* **2002**, *14*, 1067−75.

(13) Crosson, S.; Rajagopal, S.; Moffat, K. The LOV domain family: Photoresponsive signaling modules coupled to diverse output domains. *Biochemistry* **2003**, *42*, 2−10.

(14) Ditchfield, R. Hehre, W. J.; Pople, J. A. Self-consistent molecular-orbital methods. IX. An extended Gaussian-type basis for molecular-orbital studies of organic molecules. *J. Chem. Phys.* **1971**, *54*, 724−728.

(15) Ditchfield, R.; Hehre, W. J.; Pople, J. A. Self-consistent molecular orbital methods. XII. Further extensions of Gaussian-type basis sets for use in molecular orbital studies of organic molecules. *J. Chem. Phys.* **1972**, *56*, 2257−2261.

(16) Fedorov, R.; Schlichting, I.; Hartmann, E.; Domratcheva, T.; Fuhrmann, M.; Hegemann, P. Crystal structures and molecular mechanism of a light-induced signaling switch: The Phot-LOV1 domain from *Chlamydomonas reinhardtii*. *Biophys. J.* **2003**, *84*, 2474−82.

(17) Francl, M.; Pietro, W. J.; Hehre, W. J.; Binkley, S. J.; Gordon, M. S.; DeFrees, D. J.; Pople, J. A. Self-consistent molecular orbital methods. XXIII. A polarization-type basis set for second-row elements. *J. Chem. Phys.* **1982**, *77*, 3654−3665.

(18) Harper, S. M.; Neil, L. C.; Day, I. J.; Hore, P. J.; Gardner, K. H. Conformational changes in a photosensory LOV domain monitored by time-resolved NMR spectroscopy. *J. Am. Chem. Soc.* **2004**, *126*, 3390−1.

(19) Hayashi, S.; Ohmine, I. Proton transfer in bacteriorhodopsin: Structure, excitation and IR spectra, and potential energy surface analyses by an ab initio QM/MM method. *J. Phys. Chem. B* **2000**, *104*, 10678−10691.

(20) Hayashi, S.; Tajkhorshid, E.; Schulten, K. Structural changes during the formation of early intermediates in the bacteriorhodopsin photocycle. *Biophys. J.* **2002**, *83*, 1281−1297.

(21) Hegemann, P.; Fuhrmann, M.; Kateriya, S. Algal sensory photoreceptors. *J. Phycol.* **2001**, *37*, 668−676.

(22) Hertwig, R. H.; Koch, W. On the parametrization of the local correlation functional. What is Becke-3-LYP? *Chem. Phys. Lett.* **1997**, *268*, 345−351.

(23) Humphrey, W.; Dalke, A.; Schulten, K. VMD−Visual molecular dynamics. *J. Mol. Graphics* **1996**, *14*, 33−38.

(24) Iwata, T.; Tokutomi, S.; Kandori, H. Photoreaction of the cysteine S−H group in the LOV2 domain of *Adiantum* phytochrome3. *J. Am. Chem. Soc.* **2002**, *124*, 11840−1.

(25) Jarillo, J. A.; Gabrys, H.; Capel, J.; Alonso, J. M.; Ecker, J. R.; Cashmore, A. R. Phototropin-related NPL1 controls chloroplast relocation induced by blue light. *Nature* **2001**, *410*, 952−4.

(26) Kagawa, T.; Sakai, T.; Suetsugu, N.; Oikawa, K.; Ishiguro, S.; Kato, T.; Tabata, S.; Okada, K.; Wada, M. Arabidopsis NPL1: A phototropin homolog controlling the chloroplast high-light avoidance response. *Science* **2001**, *291*, 2138−41.

(27) Kalé, L.; Skeel, R.; Bhandarkar, M.; Brunner, R.; Gursoy, A.; Krawetz, N.; Phillips, J.; Shinozaki, A.; Varadarajan, K.; Schulten, L. NAMD2: Greater scalability for parallel molecular dynamics. *J. Comput. Phys.* **1999**, *151*, 283−312.

(28) Kay, C. W. M.; Schleicher, E.; Kuppig, A.; Hofner, H.; Rüdiger, W.; Schleicher, M.; Fischer, M.; Bacher, A.; Weber, S.; Richter, G. Blue light perception in plants. Detection and characterization of a light-induced neutral flavin radical in a C450A mutant of phototropin. *J. Biol. Chem.* **2003**, *278*, 10973−82.

(29) Kennis, J. T. M.; Crosson, S.; Gauden, M.; van Stokkum, I. H. M.; Moffat, K.; van Grondelle, R. Primary reactions of the LOV2 domain of phototropin, a plant blue-light photoreceptor. *Biochemistry* **2003**, *42*, 3385−92.

(30) Kinoshita, T.; Doi, M.; Suetsugu, N.; Kagawa, T.; Wada, M.; Shimazaki, K. Phot1 and phot2 mediate blue light regulation of stomatal opening. *Nature* **2001**, *414*, 656−60.

(31) Kottke, T.; Heberle, J.; Hehn, D.; Dick, B.; Hegemann, P. Phot-LOV1: Photocycle of a blue-light receptor domain from the green alga *Chlamydomonas reinhardtii*. *Biophys. J.* **2003**, *84*, 1192−201.

(32) Kowalczyk, R. M.; Schleicher, E.; Bittl, R.; Weber, S. The photoinduced triplet of flavins and its protonation states. *J. Am. Chem. Soc.* **2004**, *126*, 11393−9.

(33) Losi, A.; Kottke, T.; Hegemann, P. Recording of blue light-induced energy and volume changes within the wild-type and mutated phot-LOV1 domain from *Chlamydomonas reinhardtii*. *Biophys. J.* **2004**, *86*, 1051−60.

(34) Losi, A.; Quest, B.; Gärtner, W. Listening to the blue: The time-resolved thermodynamics of the bacterial blue-light receptor YtvA and its isolated LOV domain. *Photochem. Photobiol. Sci.* **2003**, *2*, 759−766.

(35) Neiss, C.; Saalfrank, P. Ab initio quantum chemical investigation of the first steps of the photocycle of phototropin: A model study. *Photochem. Photobiol.* **2003**, *77*, 101−9.

(36) Neiss, C.; Saalfrank, P. Molecular dynamics simulation of the LOV2 domain from *Adiantum capillus-veneris*. *J. Chem. Inf. Comput. Sci.* **2004**, *44*, 1788−93.

(37) Neiss, C.; Saalfrank, P.; Parac, M.; Grimme, S. Quantum chemical calculation of excited states of flavin-related molecules. *J. Phys. Chem. A* **2003**, *107*, 140−147.

(38) Portmann, S.; Lüthi, H. P. Molekel: An interactive molecular graphics tool. *Chimia* **2000**, *54*, 766−770.

(39) Schleicher, E.; Kowalczyk, R. M.; Kay, C. W. M.; Hegemann, P.; Bacher, A.; Fischer, M.; Bittl, R.; Richter, G.; Weber, S. On the reaction mechanism of adduct formation in LOV domains of the plant blue-light receptor phototropin. *J. Am. Chem. Soc.* **2004**, *126*, 11067−76.

(40) Schneider, C.; Sühnel, J. A molecular dynamics simulation of the flavin mononucleotide−RNA aptamer complex. *Biopolymers* **1999**, *50*, 287−302.

(41) Swartz, T. E. Corchnoy, S. B.; Christie, J. M.; Lewis, J. W.; Szundi, I.; Briggs, W. R.; Bogomolni, R. A. The photocycle of a flavin-binding domain of the blue light photoreceptor phototropin. *J. Biol. Chem.* **2001**, *276*, 36493−500.

(42) Vreede, J.; van der Horst, M. A.; Hellingwerf, K. J.; Crielaard, W.; van Aalten. D. M. F. PAS domains. Common structure and common flexibility. *J. Biol. Chem.* **2003**, *278*, 18434−9.